Determination of bond strengths of arsenic and arsenic chalcogen compounds using the temperature dependence of extended x-ray-absorption fine structure

C. Y. Yang, M. A. Paesler, and D. E. Sayers
Department of Physics, North Carolina State University, Raleigh, North Carolina 27695-8202
(Received 12 January 1987)

We present an extended x-ray-absorption fine-structure (EXAFS) study of the temperature dependence of crystalline (*c*-), As, As_2S_3, and As_4S_4, amorphous (*a*-) As, and glassy (*g*-) As_2S_3. Based on an Einstein model, we find that the mean-square relative displacement of these materials in the first shell is primarily attributable to bond-stretching modes of vibration. From a comparison with Raman spectra, it is evident that the Einstein vibrational frequencies derived from EXAFS measurements are related to the effective bond-stretching force constants. Our results indicate that As—As bonds in *c*-As are about 17% weaker than those in *a*-As. Both stretching forces of the As—S bonds in *c*- and *g*-As_2S_3 are quite similar. The calculation of bond strengths in *c*-As_4S_4 shows that As—S bonds are about 30% stronger than As—As bonds. This work underscores the fact that temperature-dependent extended x-ray-absorption fine-structure data may be used to provide information about the nature—i.e., the strength—of the local bonding.

I. INTRODUCTION

Extended x-ray-absorption fine structure (EXAFS) has been shown to be a useful tool for determining the local structure about an x-ray-absorbing atom. Many structural parameters such as interatomic distances, number of coordinating atoms, types of atoms, and relative disorder can quantitatively be obtained from experimental EXAFS spectra. In particular, it is known that the amplitude of EXAFS is damped because of disorder effects. This sensitivity to disorder can be particularly useful for obtaining information which may not be available from other techniques. The disorder effects in EXAFS can be classified as either (i) static disorder due to structural variations, (ii) dynamic disorder induced by thermal motion, or (iii) chemical disorder caused by the existence of more than one type of atom in the same shell. Measurement of the static disorder can yield important information about how much the local configurations of disordered materials may differ from their crystalline counterparts. For example, structural changes due to different preparation[1] or thermal treatment[2] of the same type of sample have been determined using structural disorder. Measurement of dynamic disorder can provide information about the local modes of vibration around the x-ray-absorbing atom. Thus measurement of the thermal disorder may permit a determination of the force constants between nearest neighbors. Chemical disorder measurements can give direct and detailed information about the local bonding of the absorbing atom.

Accurate extraction of all this information, however, depends on the methods of analyzing EXAFS data. If the disorder is small and/or Gaussian, a straightforward application of the ratio method[3] can be used. If strong interference occurs due to the contributions from different types of neighbors, the determination of structural information is more complicated. In this case, a fitting technique is usually employed. Because fitting parameters may be highly correlated, care must be taken in finding a valid fit. In some cases, this process is aided by the use of phase- and amplitude-corrected Fourier transforms[4] which were used in this analysis.

In this paper, we report an investigation of the temperature-dependent EXAFS of *c*-As (rhombohedral) and *a*-As, *c*-As_2S_3 (orpiment) and *g*-As_2S_3, and *c*-As_4S_4 (realgar). These materials are of considerable interest, and in recent years, much work has been done studying their structure using vibrational spectroscopies. In particular, their vibrational densities of states have been the subject of different experimental investigations, including ir, Raman, and inelastic neutron scattering. Numerous theoretical models have been proposed for these materials. A major feature of these solids is that their local bonding structures are based on molecular units and that their optic-mode frequencies are dominated by short-range interactions.

An important issue is what microscopic physical parameters can be determined from the temperature dependence of the EXAFS. In current EXAFS theories it is assumed that the mean-square relative displacement (MSRD) is related to a local, projected density of modes.[5] Since EXAFS is sensitive only to relative motion along the bond directions, a strong correlation should exist between the mean-square displacement and the optical phonon spectrum, so that the main contributions to the MSRD should come primarily from optical phonons. Our study suggests that the thermal vibration of pairs of atoms in the first shell of these materials is presumably related to the bond-stretching modes. Hence, temperature-dependent EXAFS studies can be used as a quantitative assessment of bond strength in these materials. The purpose of this paper is to determine the MSRD induced by the thermal motion of atoms to relate these results to the bond strengths in these materials in Sec. II, we describe the structure of the samples. In Sec. III, we present experimental details. In Sec. IV, we explain the data

analysis. In Sec. V, we discuss the interpretation of the results based on the Einstein model and compare them to Raman spectra to determine the local modes of vibration for the As—S and As—As bonds. From these results a determination of the bond strength is made. We conclude in Sec. VI.

II. STRUCTURE

Rhombedral *c*-As consists of double layers extended in a two-dimensional network of sixfold rings of atoms. Each As atom has three nearest neighbors within a layer and three weakly bonded next-nearest neighbors in adjacent layers. In this structure, triangular pyramids as basic units are linked to form covalently bonded layers. The structure of *a*-As and its relation to *c*-As have been discussed by Greaves *et al.*[6] The local structure of *a*-As is very similar to *c*-As with respect to the first-neighbor coordination, bond distances, and angles. The structural differences arise mainly from the manner in which arsenic pyramids are linked and are important for third or higher neighbors.

The crystal structure of orpiment[7] is layered with spiral chains of S-As-S-As running parallel to the *c* axis. The layers are arranged normal to the *b* axis. Each layer contains twelve-membered rings of atoms with alternative As and S atoms. The layers are believed to be held together by weak van der Waals forces. Each As atom is bonded to three S atoms forming strong covalent bonds in a triangular pyramidal arrangement with the As atom at the apex and the three S atoms[8–10] forming the base. The AsS_3 pyramids are linked together by As—S—As bonds. Results of x-ray and neutron scattering, ir and Raman spectra are in agreement in concluding that the short-range order of the crystal is preserved in glassy As_2S_3. That is, first- and second-neighbor distances and coordination numbers are approximately the same.

Realgar is built from separate cagelike As_4S_4 molecules[11] held together by van der Waals forces. The four S and four As atoms in the molecule are covalently bonded together to form a square and a tetrahedron, respectively. Each As is bonded to three nearest neighbors, two sulfur atoms, and an arsenic atom. An important feature of all of these materials is that their local structures are based on molecular units.

III. EXPERIMENTAL DETAILS

Natural crystals of As_2S_3 and As_4S_4 were obtained from Ward's Natural Science Establishment. The rhombohedral (99.999%) and *a*-As (99.9999%) were obtained from Atomergic Chemetals. The crystallinity of *c*-As_2S_3 and *c*-As_4S_4 samples was confirmed by x-ray diffraction. Lattice parameters were matched with known crystalline spectra. The composition of the samples was analyzed in an electron microscope using an energy dispersive spectrometer. No detectable impurities were seen at the sensitivity limit of the analysis (0.2% by weight). Samples of 99.999% pure *a*-As_2S_3 were placed into quartz tubes which were sealed under a vacuum of 10^{-6} torr. These were heated in a rocking furnace for 24 h at 650 °C and ice quenched before being returned to room temperature. These samples were separately ground to fine powders and placed on Kapton tape for EXAFS measurements.

The EXAFS measurements were performed at the National Synchrotron Light Source (NSLS) on the X-11 beam line with a Si(111) double crystal monochromator. The data were consistent during several different runs. Measurements were made on *c*-As, *c*-As_2S_3, and *c*-As_4S_4 at 15, 80, 145, and 300 K. The samples were oriented for x-ray transmission and attached to a sample holder mounted on a displex cryostat. The *a*-As and *g*-As_2S_3 samples were measured at 80 K and room temperature only.

In order to avoid thickness effects (an important source of error in the measurement of the Debye-Waller term), various thicknesses were measured. All of the uniform samples used in this work had an edge step of $\Delta(\mu x) < 1.1$ which is lower than the theoretical optimum[12] so that the EXAFS does not change for different thicknesses. The monochromator crystals were detuned, reducing the diffracted intensity by 20% in order to reduce the harmonic content of the beam. Three ionization chambers filled with appropriate gases were used to measure x-ray intensities. *c*-As was placed before the third ionization chamber to provide simultaneous calibration of the edge energy.

IV. DATA AND ANALYSIS

The EXAFS data were extracted using standard techniques[13] of background subtraction and normalization. The resulting EXAFS $\chi(k)$ weighted by k^3 are shown in Fig. 1. The magnitude of the Fourier transform of the EXAFS data shown in Fig. 2 were obtained by multiplying the EXAFS data by k^3 and transforming over a *k*-space range of 2.5 to 15.8 Å^{-1}.

By making a number of approximations,[14] structural information contained in the EXAFS interference function can be described as

$$\chi(k) = -\sum \frac{N_i}{kR_i^2} F_i(k) e^{-2R_i/\lambda} e^{-2\sigma_i^2 k^2} \times \sin[2kR_i + \phi_i(k)] , \quad (1)$$

where the sum is over coordination shells at an average distance R_i from the absorbing atom, and N_i is the number of scattering atoms in the ith shell at distance R_i. The electron wave vector is defined as $k = [2m(E - E_0)/\hbar]^{1/2}$, where E is the photon energy, while E_0 and m are the threshold energy and mass of the electron, respectively. $F_i(k)$ is the magnitude of the backscattering and is a function of the type of scattering atom. $\phi_i(k)$ is a phase shift produced by the interaction of the photoelectron with the potentials of the central and backscattering atoms. σ_i^2 is the mean-square deviation from the average distance between the origin atom and scattering atom. The factor σ_i^2 contains contributions from both structural disorder and thermal motion of the atoms in a given shell. Structural disorder can be due either to a single site with different bond lengths or an ensemble of different sites. In principle, static structural and thermal

vibrational disorder can be separated by measuring EXAFS at various temperatures. This type of damping term $e^{-2\sigma^2 k^2}$ is only appropriate in the case of a small Gaussian disorder when $\sigma^2 k^2 \ll 1$.[15]

Using standard techniques, a single shell of the EXAFS can be isolated by Fourier filtering, and its phase and amplitude are determined as functions of k. From Eq. (1) the amplitude of this envelope function is determined by the number of neighbors N, the backscattering amplitude $F(k)$, and the Debye-Waller factor σ^2. In our study, since the environments of As atoms are the same for both the samples and standards, N and $F(k)$ should be the same, and differences in the envelope function should be due only to differences in σ^2. For c-As, a-As, c-As_2S_3, and g-As_2S_3, Debye-Waller factors are determined by plotting the logarithm of the ratio of the first shell amplitude of each sample at different temperatures T_1 and T_2. Assuming a small thermal expansion, we obtain

$$\ln[\chi(T_2)/\chi(T_1)] = 2k^2[\sigma^2(T_1) - \sigma^2(T_2)] \ . \quad (2)$$

A plot of the logarithm of the ratio of the amplitude versus k^2 yields a straight line with slope $2[\sigma^2(T_1) - \sigma^2(T_2)]$. Any significant deviation from

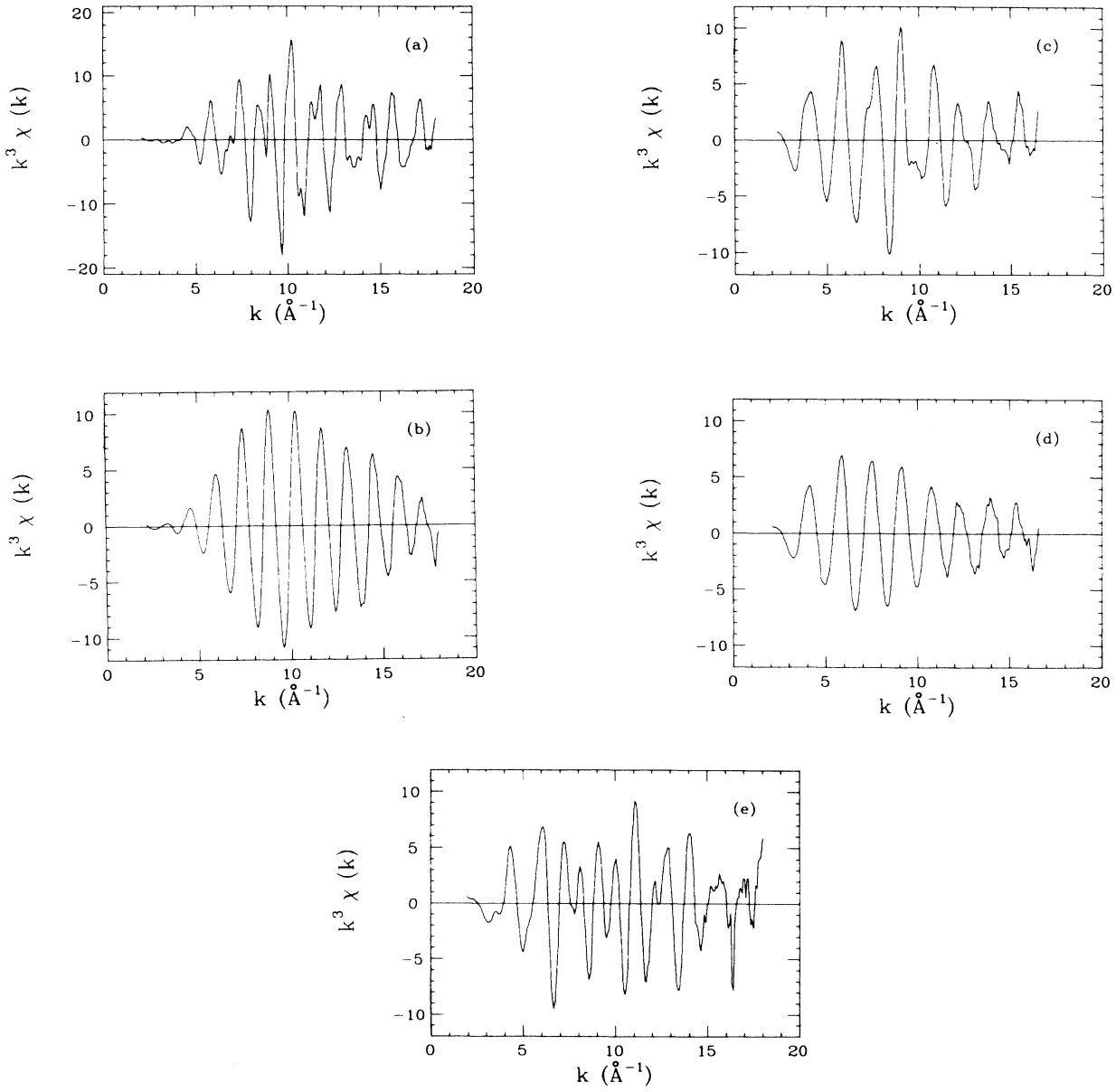

FIG. 1. EXAFS, $k^3\chi$, for (a) c-As, (b) a-As, (c) c-As_2S_3, (d) g-As_2S_3, and (e) c-As_4S_4. The c-As, c-As_2S_3, and c-As_4S_4 were measured at 15 K; the a-As and g-As_2S_3 were measured at 80 K.

linearity is indicative of either (a) more than one type of atom in the shell being studied, (b) large, non-Gaussian disorder, (c) systematic errors induced by the analysis, or (d) poor signal-to-noise ratio due to experimental or statistical errors. A representative plot for c-As is shown in Fig. 3.

Due to the strong interference between the signal of the two As—S bonds and the one As—As bond in the c-As_4S_4, it is impossible to separate each contribution from an inverse Fourier transformation as shown in Fig. 4(a). In this case, the approach is to analyze filtered data by nonlinear least-squares fitting using appropriate reference compounds for the backscattering amplitudes and phases. This analysis was also aided by the use of phase-corrected Fourier transforms which were useful in demonstrating that a complete and accurate separation of the individual

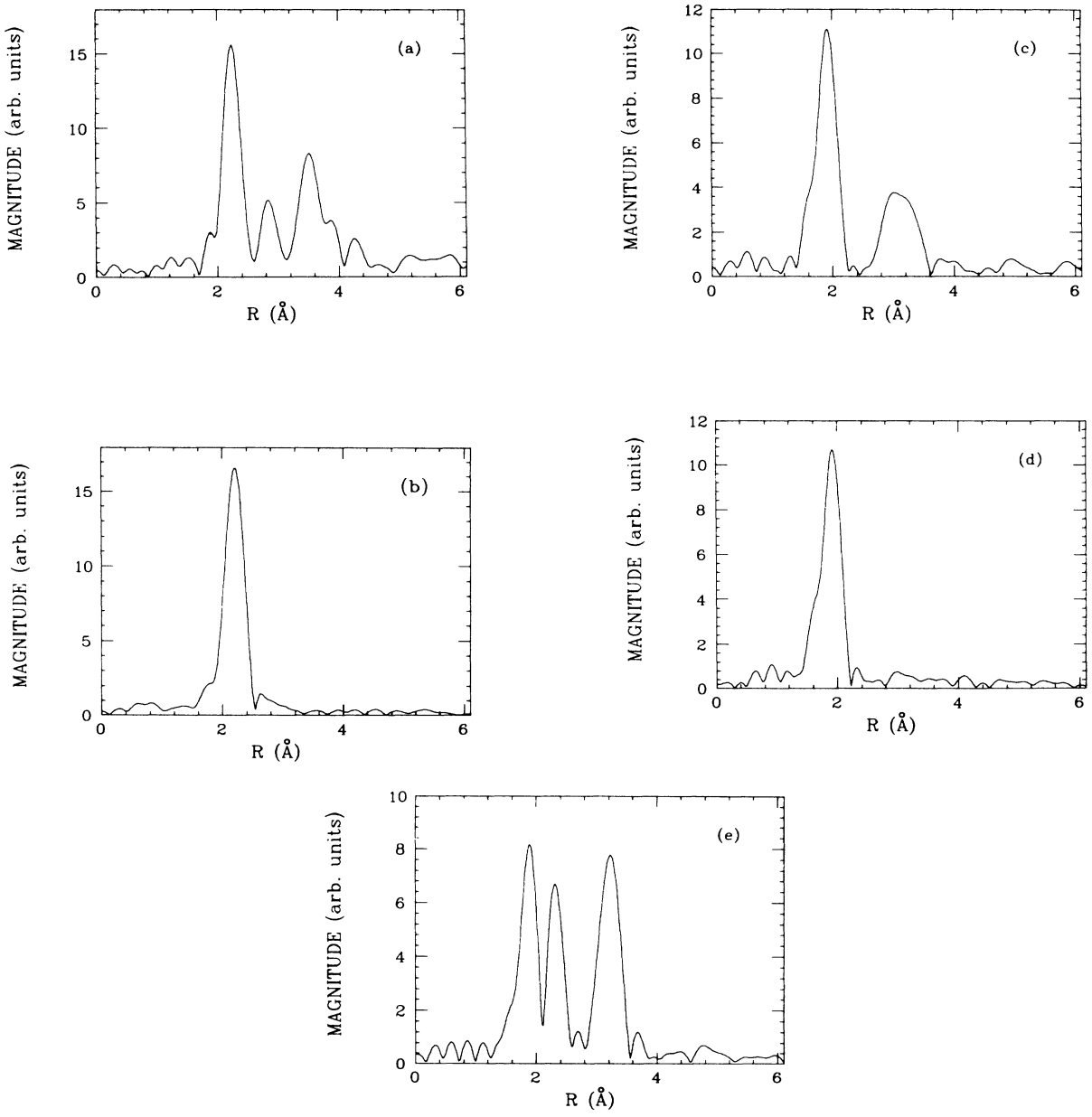

FIG. 2. The magnitude of the Fourier transforms weighted by $k^3\chi(k)$ over the range 2.5 to 15.8 Å^{-1} for (a) c-As, (b) a-As, (c) g-As_2S_3, (d) g-As_2S_3, and (e) c-As_4S_4. As expected, the Fourier transform of c-As shows that the first major peak is due to the contributions from three neighbors at 2.51 Å within a layer and the first peak of Fourier transform for a-As is due to a slightly different bond distance of 2.49 Å. The Fourier transforms of c- and g-As_2S_3 show that the first major peaks are due to the contributions from three As—S bonds forming the AsS_3 pyramids at 2.25 Å. The Fourier transform c-As_4S_4 shows two major peaks, the first one is due to the contributions of two As—S bonds at 2.24 Å and the other one is due to the contribution from one As—As bond at 2.57 Å.

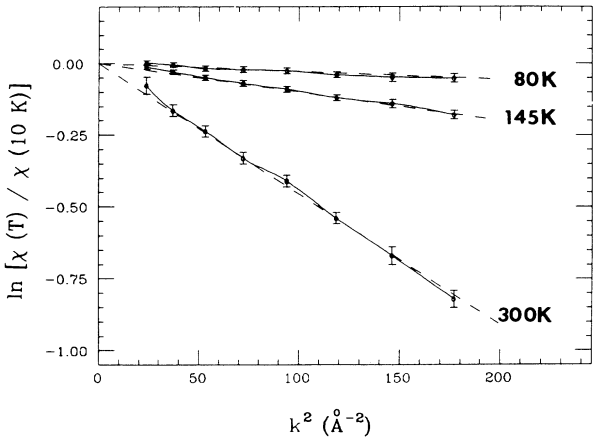

FIG. 3. The logarithm of the ratio of the isolated first-shell EXAFS amplitudes vs k^2 for c-As at 80, 145, and 300 K. The data of c-As at 15 K was used as a standard. The temperature dependence of the MSRD in c-As were determined using the straight dashed lines which were obtained by fitting to the data.

contributions were achieved. This is done by using the symmetry of the imaginary part after a phase-corrected Fourier transform as a criterion for each type of scattering atom which contribute to the EXAFS spectrum in the region of r space being analyzed.

We fit the inverse Fourier transform of the data over a range from 4 to 14.4 Å^{-1} with a two-shell model. Because of the good signal-to-noise ratio, the best fits were obtained by using k^3 weighting. Fitting was done using empirical amplitudes and phases determined from c-As_2S_3 and c-As for As—S and As—As, respectively. In order to test the structural parameters determined from the k-space fitting, the contribution of each pair of atoms in the same shell were subtracted from the measured spectrum using the fitting parameters. Then, the phase corrected Fourier transform was applied to each of the residual spectra. In this method the residual EXAFS spectrum is transformed after first multiplying the spectrum by $\exp[-i\phi(k)]$, where $\phi(k)$ is the empirically derived phase from the standard compounds. If only one type of scatterer remains, this phase-corrected Fourier transform should only show a single peak with a symmetric imaginary part whose maximum coincides with the maximum of the transform magnitude. This is demonstrated in Figs. 4(b) and 4(c). Figure 4(b) shows only the contributions of two As—S bonds obtained by subtracting the As—As contribution obtained from the fitting results, viz., $N_{\mathrm{As-As}}=1$, $R_{\mathrm{As-As}}=2.57$ Å, $\Delta\sigma^2=-0.00067$ Å^2, $\Delta E_0=-0.15$ eV. In the same way, Fig. 4(c) shows the residual phase-corrected Fourier transform containing the contribution of the As—As bonds by subtracting the contribution of As—S bonds using the fitting parameter values: $N_{\mathrm{As-S}}=2$, $R_{\mathrm{As-S}}=2.24$ Å, $\Delta\sigma^2=-0.00021$ Å^2, $\Delta E_0=-0.20$ eV. Though some small deviation still exists, the imaginary part of the residual phase-corrected Fourier transforms are nearly symmetric, indicating a reliable analysis has been achieved.

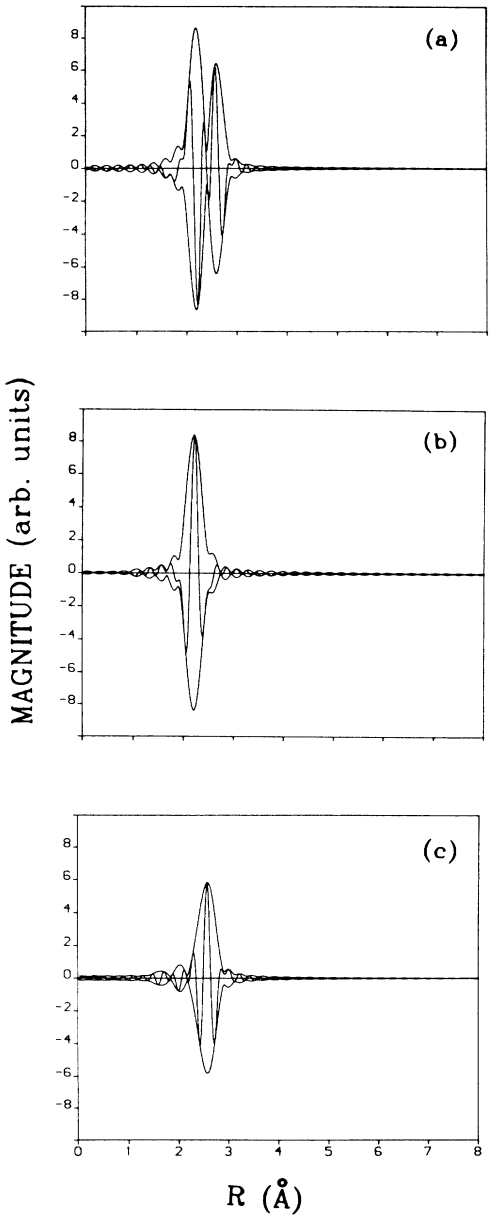

FIG. 4. The imaginary part and the magnitude of the Fourier transforms $k^3\chi(k)$ of the isolated first shell for c-As_4S_4 at 15 K. All transforms are done over a k space range of 2.5 to 15.8 Å^{-1} for (a) without phase correction, (b) As—S phase-corrected residual spectra of only the As—S contribution, and (c), As—As phase-corrected residual spectra of only the contribution due to a single As—As bond. In (b) and (c) the residual spectra due to two As—S bonds one As—As bond were found using fitting results.

V. RESULTS AND DISCUSSION

A. The Einstein model

Calculation of the appropriate MSRD for many solids is complicated when the materials have low symmetry. It may also be difficult when there is a lack of knowledge of

the phonon spectrum of the solid. In materials such as amorphous and glassy semiconductors, there is not an exact method to calculate the thermal disorder for each shell. However, the thermal vibrational behavior of solids can be determined, in part, from a measurement of the temperature dependence of the EXAFS. The MSRD, σ_i^2, is also commonly referred to as a Debye-Waller factor. It should be noted that the Debye-Waller factor as determined by EXAFS differs from that obtained by x-ray diffraction. The latter factor refers to the absolute root-mean-square displacement of an individual atom, while the EXAFS Debye-Waller factor refers to the root-mean-square relative displacement along the bond direction between the absorbing and backscattering atom. The shell-to-shell variation in σ_i^2 (Ref. 16) can be described by relating it to the individual motion of the absorbing and scattering atoms,

$$\sigma_i^2 = \langle [(\mathbf{u}_i - \mathbf{u}_0)\cdot\hat{\mathbf{R}}_i]^2 \rangle \ , \tag{3}$$

where $\mathbf{u}_i$ and $\mathbf{u}_0$ are the ith atom and central-atom displacement vectors, $\hat{\mathbf{R}}_i$ is a unit vector in the direction $\mathbf{R}_i - \mathbf{R}_0$, and the brackets refer to a thermal average. For atomic motions that are completely uncoupled, σ_i^2 approaches $\langle (\mathbf{u}_0\cdot\hat{\mathbf{R}}_i)^2 \rangle + \langle (\mathbf{u}_i\cdot\hat{\mathbf{R}}_i)^2 \rangle$. When the motions are correlated, the cross term, $2\langle (\mathbf{u}_0\cdot\hat{\mathbf{R}}_i)(\mathbf{u}_i\cdot\hat{\mathbf{R}}_i) \rangle$, is important, especially for nearest-neighbor atoms. This emphasizes the fact that σ_i^2 is shell dependent and thus depends on the structure and force constants of the material.

There are two approximations for determining the thermal vibrational contribution to $\sigma_i^2(T)$. According to Rehr,[5] the Einstein approximation is superior to the Debye approximation for the first shell. This has been verified by Bunker[17] who has found that the values of MSRD in the first shell for various materials are much closer to the Einstein approximation than to the Debye approximation. Because the short-range correlation of motion is due to high phonon wave vectors and the long-range correlation is due to low phonon wave vectors, the contribution of the phonon spectrum to the MSRD in the first shell is dominated by the optical modes. In the Einstein approximation,[18] the phonon density of modes is approximated by a δ function at a single frequency, and therefore, the $\sigma_i^2(T)$ of EXAFS can be written;[5]

$$\sigma_i^2(T) = \frac{\hbar}{2\mu\omega_E} \coth\left[\frac{\hbar\omega}{2k_B T}\right] , \tag{4}$$

where μ is the reduced mass, k_B is the Boltzmann's constant, and ω_E is the Einstein frequency. Later, we will use the fact that ω_E can be also estimated from vibrational spectroscopies. To compare with experiment, which measures $\Delta\sigma_i^2(T)$, Eq. (4) is modified to

$$\Delta\sigma_i^2 = \frac{\hbar}{2\mu\omega_E}\left[\coth\left[\frac{\hbar\omega}{2k_B T_2}\right] - \coth\left[\frac{\hbar\omega}{2k_B T_1}\right]\right] . \tag{5}$$

A comparison of the calculated results from the Einstein model and the experimental data is shown in Fig. 5.

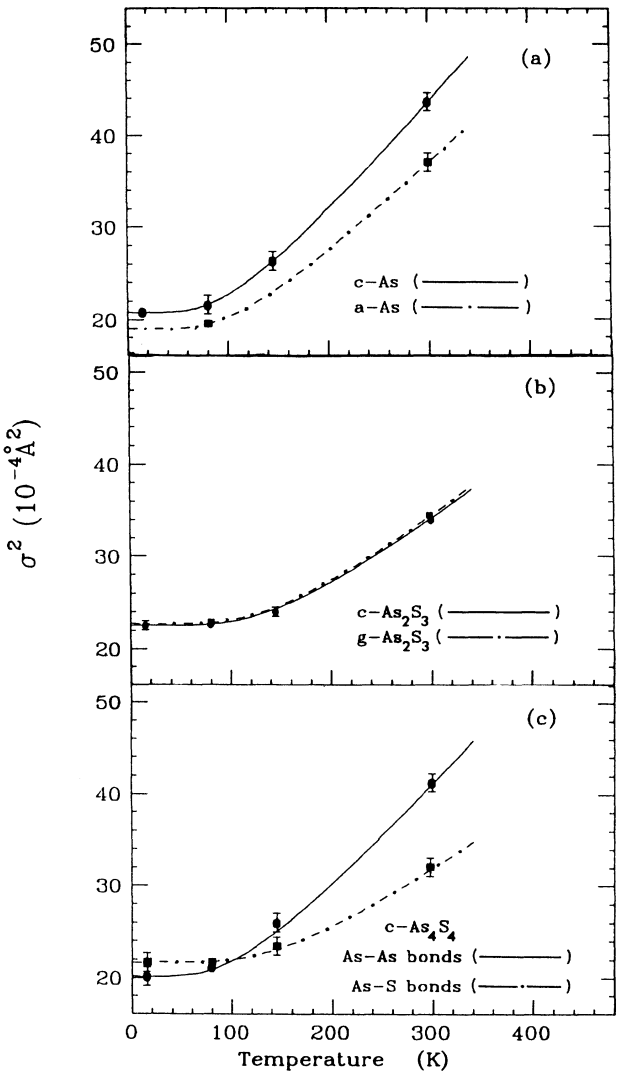

FIG. 5. Changes with temperature of the MSRD, σ^2, of the first shells for (a) As—As bonds in c- and a-As, (b) As—S bonds in c- and g-As_2S_3, and (c) As—As and As—S bonds in c-As_4S_4. The solid and dashed lines represent the Einstein model calculations for the c- and a- materials, respectively.

B. Comparison with Raman spectroscopy

Although the advantage of taking EXAFS data at low temperatures has been recognized for years, the interpretation of the experimental results has received considerably less attention. In order to use the temperature dependence of the EXAFS to extract microscopic physical parameters we have found[19] it fruitful to compare our data with Raman spectra of the same samples. Since EXAFS is sensitive only to the local atomic environments of an absorbing atom, it has been suggested[5] that the Debye-Waller factor in EXAFS is related to a projected local density of modes. If we assume that the motion of neighboring atoms is uncorrelated, the projected density of states of modes deduced from EXAFS is directly pro-

portional to the vibrational total density of modes. Therefore, there is a close connection between EXAFS measurements and the reduced Raman intensity. This conjectured relationship between the projected density of modes in EXAFS and Raman intensity has been demonstrated by Lottici and Rehr.[20] In this paper, we concentrate only on understanding the important features of the temperature dependence of the EXAFS without attempting a detailed calculation of the local density of vibrational modes. The simplest understanding of the thermal motion of a pair of atoms in these materials is based on assuming only central nearest-neighbor interactions with one effective spring constant. For those materials for which approximation is adequate, the Einstein model leads easily to identification of the vibrational spectra of normal modes in terms of contributions from specific pairs of atoms.

For the systems we are studying, one of our primary concerns is local stretching modes associated with the As—S and As—As bonds. A comparison of the Einstein vibrational frequency, in wave numbers, $\nu_E = \omega_E / 2\pi c$, derived from EXAFS and the vibrational frequency derived from Raman spectra is shown in Table I. It can be seen that the Einstein vibrational frequencies determined from EXAFS are quite close to the symmetrical-stretching-mode frequencies ν_s. The magnitude of the difference between ν_E and ν_s is less than 10%. Our results demonstrate that the MSRD is dominated by the optical stretching modes while any bending modes which occur at lower frequencies, as well as any acoustic modes, do not contribute to the MSRD.

Much of the discrepancy between ν_E and ν_s, shown in Table I, is due to the fact that ν_E is determined by the average phonon properties which includes contributions from both the symmetric and antisymmetric modes. These, in turn, depend on the structure of the material. For example, based on Herzberg's[26] mode analysis of a regular pyramidal molecule, an improved agreement between ν_E and ν_s can be achieved by correctly relating ν_E to a combination of symmetric and antisymmetric frequencies. This will be shown in detail in a later paper.[27]

For the case of rhombohedral As, the two phonon bonds measured from inelastic neutron scattering[28] are centered around 95 and 205 cm^{-1}. Information about the density of states may be obtained by comparison between Raman[21] and neutron measurements. The two principal bands are attributed to the three acoustic and three optical modes characteristic of the rhombohedral structure. For a-As, the upper-mode peak is centered around 235 cm^{-1}. The optical-mode frequencies based on the normal modes of the As_4 molecules[22] are determined primarily by the short-range interatomic forces. Therefore, the bond-stretching modes corresponding to As—As bond-stretching vibrations in c-As and a-As can be easily identified from EXAFS measurements.

The main vibrational band of c-As_2S_3 has three stretching modes at 309, 354, and 383 cm^{-1}.[23] The highest mode at 383 cm^{-1} which is responsible for the interaction between pyramidal units gives a much smaller contribution to the EXAFS. The other two modes which are attributed to the stretching within a pyramidal unit make the primary contribution to the MSRD. As mentioned in Sec. II, AsS_3 pyramidal units exist in both glassy and crystalline As_2S_3. Lucovsky and Martin[10] first proposed a molecular model based on the local atomic arrangement to explain the optical spectra of g-As_2S_3. In their model the dominant Raman active mode is the symmetric ν_1 mode at 340 cm^{-1} and the dominant ir active mode is the antisymmetric ν_3 mode at 310 cm^{-1}. From our EXAFS results, it is evident that ν_E can be interpreted as the average of the stretching-mode frequencies. The values of ν_E for c- and g-As_2S_3 are identical, within the error, which suggests that both main stretching modes of c- and g-As_2S_3 are similar. This is in good agreement with the calculation of DeFonzo and Tauc.[29]

In the case of realgar, the problem of assigning the As—As stretching modes to the Raman peaks is still not resolved.[30,31] The reason for this is that the cage model of c-As_4S_4, according to the selection rules, places the As—As stretching frequencies as well as the As—S bending modes, around 220 cm^{-1}. Therefore, it is difficult to identify which of the particular features in the Raman spectrum in the band between 140 and 230 cm^{-1} are due to the As—As stretching modes. The EXAFS results suggest that the feature at 222 cm^{-1} should be assigned to the average As—As stretching mode in which the pair of arsenic atoms, on the same side of the equatorial plane

TABLE I. Comparison of the Einstein vibrational frequencies ν_E and Raman symmetrical stretching frequencies ν_s in arsenic and arsenic-chalcogen compounds. The asterisk indicates that the error in the listed values were estimated from systematic errors in the analysis.

Material	Bond	ν_E (cm^{-1})	ν_s (cm^{-1})
c-As	As—As	216±5*	205[a]
a-As	As—As	234±5	235[b]
c-As_2S_3	As—S	332±5	354[c]
g-As_2S_3	As—S	330±5	340[d]
c-As_4S_4	As–As	222±10	220[e]
	As—S	342±10	354[e]

[a]Reference 21.
[b]Reference 22.
[c]Reference 23.
[d]Reference 24.
[e]Reference 25.

formed by the four sulfur atoms, move away from each other. Since EXAFS is sensitive to relative correlated motion of pairs of atoms and the bond angles of c-As_4S_4 are all nearly 90°, other contributions to the MSRD will be less when the movement of the pair of arsenic atoms is in phase. The mode at 346 cm^{-1} arises from the average As—S stretching modes of the triangle of As atoms with respect to the attached sulfur atoms. The above assignment is consistent with the feature in the Raman spectrum at 354 cm^{-1}. The strongest band at 354 cm^{-1} is due to the totally symmetric vibration of the covalently bonded S-As-S-As spiral.

C. Determination of the bond strengths

Traditionally, there are two approaches for estimating force constants; one is using Gordy's rule[32] and the other is to scale the frequencies from the reported vibrational frequencies of molecules with similar structure and mass ratios. In this work we report a new direct, empirical way to estimate the force constants.

The effective bond-stretching force constant can be derived from the vibrational frequencies determined from the EXAFS using the following relationship:

$$f_E = 4\pi^2 c^2 \mu \nu_E^2 \ . \tag{6}$$

A comparison of observed f_E from EXAFS and the force constants f_G derived from Gordy's rule is given in Table II. The values are quite different. This is not surprising since Gordy's rule is an empirical relation used to describe bonding trends in families of materials. For example, Hilton *et al.*[33] find large discrepancies using Gordy's rule to calculate bond distances for As_2S_3 and As_2Se_3 glasses. Our results are more direct and should, therefore, provide better values for the bond-stretching force constants.

Some points, however, are worth mentioning. From Fig. 5, it can be seen that $\Delta\sigma_i^2$ changes very little below 80 K. The reason for this is clear; the MSRD is related to the mean potential energy of an oscillator at low temperature which is determined by the zero-point vibrations. For a material with strong bonding, the phonons are in the ground state at low temperature where the zero-point motion, σ_0^2, can be treated as a simple harmonic motion. Hence, σ_0^2 should depend only on the masses and force constant so that it also provides a check on the calculated bond strength.

TABLE II. Comparison of bond-stretching force constants.

Sample	Bond	(EXAFS Measurements) f_E (10^5 dyn/cm)	(Gordy's Rule) f_G (10^5 dyn/cm)
c-As	As—As	1.03	1.49
a-As	As—As	1.21	1.50
c-As_4S_4	As—As	1.09	1.43
c-As_2S_3	As–S	1.46	1.97
a-As_2S_3	As–S	1.44	1.97
c-As_4S_4	As–S	1.59	1.97

The ratio of the effective bond-stretching force constants between a- and c-As is about 1.17. That is, the As–As bonds in c-As are about 17% weaker than those in a-As. This weakening of the As—As bond in c-As is most likely due to the mixture of metallic and covalent bonding which results in a longer bond distance. The calculation of the bond strengths of the homopolar and heterpolar bonding in c-As_4S_4 shows that As—S bonds are about 30% stronger than the As—As bonds.

VI. CONCLUSION

The success of our approach owes much to the fact that beyond the nearest neighbors the motion of other atoms is uncorrelated due to the strong central forces within the molecular units and the fact that the bonds angle nearly 90° in these materials. The analysis of the bond strengths will become more complicated in compounds where intermolecular interactions are also important or strong collective effects contribute to the lattice vibrations. Then an exact determination of bond strength will involve a theoretical calculation. Nevertheless, if the thermal vibrational behavior of pairs of atoms are approximately harmonic, this method might still be useful to provide a rough estimate of the bond strength.

The main result of our study is the demonstration that the measurements of temperature dependence of EXAFS provide a way to determine local bond-stretching vibrations. Our results, based on the Einstein model, clearly show that the MSRD in EXAFS is dominated by the optical stretching modes. The agreement between the EXAFS and Raman measurements is quite respectable.

Although the temperature dependence of EXAFS cannot provide the same insight and detail about the local modes of vibrational that Raman measurements it gives an easy way to identify the main bond-stretching modes. A strength of the EXAFS technique is its ability to determine the local dynamical motion about each type of atom in a variety of forms, for example, when only a small amount of powder is available or for highly disordered or dilute samples for which traditional vibrational techniques are difficult.

The applicability of this method has been demonstrated using arsenic and arsenic-chalcogen compounds. Differences in bond strengths for particular bonds were found depending on the materials or environment. We plan to extend this method to other problems such as variations in bond strength which could occur as a function of composition or thermal and photoinduced effects.

ACKNOWLEDGMENTS

One of us (C.Y.Y.) wishes to thank D. C. Koningsberger and J. M. Tranquada for helpful discussions. Support for the development of beamline X-11A at NSLS and partial support for this research was provided by the Department of Energy under Contract No. DE-AS05-80ER10742. Partial support for this research was also provided by the National Science Foundation under Grant No. DMR-8407265.

[1]C. Y. Yang, M. A. Paesler, and D. E. Sayers. Mater. Lett. **4**, 233 (1986).
[2]M. A. Paesler, D. E. Sayers, R. Tsu, and J. G. Hernandez, Phys. Rev. B **28**, 4550 (1984).
[3]D. E. Sayers, F. W. Lytle, and E. A. Stern, Phys. Rev. B **11**, 4836 (1975).
[4]J.B.A.D. Van Zon, D. C. Koningsberger, R. Prins, and D. E. Sayers, in *EXAFS and Near Edge Structure III,* edited by K. O. Hodgson, B. Hedman, and J. E. Penner-Hahn (Springer-Verlag, New York, 1984).
[5]J. J. Rerh (unpublished).
[6]G. N. Greaves, S. R. Elliot, and E. A. Davis, Adv. Phys. **28**, 49 (1978).
[7]N. Morimoto, Mineral. J. (Sapporo) **1**, 160 (1954).
[8]A. Vaipolin and C. A. Porai-Koshitz, Fiz. Tverd. Tela (Leningrad) **5**, 246 (1963).
[9]P. C. Taylor, S. G. Bishop, and D. L. Mitchell, Phys. Rev. Lett. **27**, 414 (1971).
[10]G. Lucovsky and R. M. Martin, J. Non-Cryst. Solids **8**, 185 (1971).
[11]P. J. Mullen and W. Nowacki, Z. Kristallogr. Mineral. **136**, 48 (1972).
[12]E. A. Stern and K. Kim, Phys. Rev. B **23**, 3781 (1981).
[13]J. W. Cook, Jr. and D. E. Sayers, J. Appl. Phys. **52**, 5024 (1981).
[14]E. A. Stern, Phys. Rev. B **10**, 3027 (1974).
[15]G. B. Bunker, Nucl. Instrum. Methods **207**, 437 (1983).
[16]G. Beni and P. M. Platzmann, Phys. Rev. B **14**, 1514 (1976).
[17]B. A. Bunker, Ph.D. Thesis, University of Washington, 1980 (unpublished).
[18]E. Sevillano, H. Meuth, and J. J. Rehr, Phys. Rev. B **20**, 4908 (1979).
[19]C. Y. Yang, M. A. Paesler, and D. E. Sayers J. Phys. (Paris) Colloq. **47**, C8-391 (1986).
[20]P. P. Lottici and J. J. Rerh, Solid State Commun. **35**, 565 (1980).
[21]J. S. Lannin, J. M. Callega, and M. Cardona, Phys. Rev. B **12**, 585 (1975).
[22]J. S. Lannin, Phys. Rev. B **15**, 3863 (1977).
[23]R. J. Koblisa and S. A. Solin, Phys. Rev. B **8**, 756 (1973).
[24]A. T. Ward, J. Phys. Chem. **72**, 4133 (1968).
[25]R. Zallen and M. L. Slade, Phys. Rev. B **18**, 5775 (1978).
[26]G. Herzberg, *Infrared and Raman Spectra of Polyatomic Molecules* (Van Nostrand Reinhold, New York, 1945).
[27]J. M. Tranquada and C. Y. Yang (unpublished).
[28]A. J. Leadbetter, D. M. Smith, and P. Sefyert, Philos. Mag. **33**, 441 (1976).
[29]A. P. DeFonzo and J. Tauc, Phys. Rev. B **18**, 6957 (1978).
[30]R. Forneris, Am. Mineral. **54**, 1062 (1969).
[31]W. Scheurmann and G. J. Ritter, Z. Naturforsch. **24A**, 408 (1969).
[32]W. Gordy, J. Chem. Phys. **5**, 345 (1946).
[33]A. R. Hilton, C. E. Jones, R. D. Dobrott, H. M. Klein, A. M. Byrand, and T. D. George, Phys. Chem. Glasses **7**, 116 (1966).